

## A POSSIBLE $\sim 20$ -YEAR PERIODICITY IN LONG-TERM VARIATIONS OF THE NEARBY RADIO-QUIET ACTIVE GALACTIC NUCLEUS ARK 120

YAN-RONG LI<sup>1</sup>, JIAN-MIN WANG<sup>1,2,3</sup>, ZHI-XIANG ZHANG<sup>1</sup>, KAI WANG<sup>1</sup>, YING-KE HUANG<sup>1</sup>, KAI-XING LU<sup>4</sup>, CHEN HU<sup>1</sup>, PU DU<sup>1</sup>,  
LUIS C. HO<sup>5,6</sup>, JIN-MING BAI<sup>4</sup>, WEI-HAO BIAN<sup>7</sup>, YE-FEI YUAN<sup>8</sup>

<sup>1</sup>Key Laboratory for Particle Astrophysics, Institute of High Energy Physics, Chinese Academy of Sciences,  
19B Yuquan Road, Beijing 100049, China; [liyanrong@mail.ihep.ac.cn](mailto:liyanrong@mail.ihep.ac.cn), [wangjm@mail.ihep.ac.cn](mailto:wangjm@mail.ihep.ac.cn)

<sup>2</sup>National Astronomical Observatories of China, Chinese Academy of Sciences, 20A Datun Road, Beijing 100020, China

<sup>3</sup>School of Astronomy and Space Science, University of Chinese Academy of Sciences, 19A Yuquan Road, Beijing 100049, China

<sup>4</sup>Yunan Observatories, Chinese Academy of Sciences, Kunming 650011, Yunan, China

<sup>5</sup>Kavli Institute for Astronomy and Astrophysics, Peking University, Beijing 100871, China

<sup>6</sup>Department of Astronomy, School of Physics, Peking University, Beijing 100871, China

<sup>7</sup>Physics Department, Nanjing Normal University, Nanjing 210097, China

<sup>8</sup>Department of Astronomy, University of Science and Technology of China, Hefei 230026, China

*submitted to The Astrophysical Journal Letter*

### ABSTRACT

We report a possible periodicity in the long-term monitoring of Ark 120, a nearby radio-quiet active galactic nucleus (AGN) at a distance of 143 Mpc ( $z = 0.03271$ ). We compile the historic archival photometric and spectroscopic data of Ark 120 since 1974 and make a new two-year monitoring campaign in 2015-2017, leading to a total temporal baseline over four decades. The long-term variations in continuum exhibit a sinusoidal pattern with a period of  $\sim 20$  years and the  $H\beta$  integrated flux series varies with a similar pattern. The broad  $H\beta$  profiles have asymmetric double peaks, which vary strongly with time in both amplitudes and separations and tend to shift and merge into a single peak during some epochs. Ark 120 is one of the nearest radio-quiet AGNs with periodic variability and therefore is a plausible candidate for sub-parsec supermassive black hole binaries. The present database covers two cycles of the period and it is highly worthy of continued monitoring of Ark 120 to track more cycles to study the origin of the periodicity in general and the processes related with supermassive black hole binaries in particular. The supermassive black hole binary system in Ark 120 is possibly spatially resolved by the Event Horizon Telescope and its gravitational wave radiation lies within the sensitivity of next-generation Pulsar Time Array.

*Subject headings:* galaxies: active — galaxies: individual (Ark 120) — quasars: general — methods: data analysis — methods: statistical

### 1. INTRODUCTION

Periodic brightness variability in long-term monitoring of active galactic nuclei (AGNs) is widely used to search for supermassive black hole binary candidates in modern time-domain surveys (e.g., [Graham et al. 2015a,b](#); [Liu et al. 2015, 2016](#); [Charisi et al. 2016](#); [Zheng et al. 2016](#)). Although there exist alternative explanations, such a periodicity is generally believed to signalize the binary's orbital motion, which modulates accretion processes into the black holes, giving rise to periodic variations in disk emissions. To date systematic searches from large surveys have yielded more than one hundred of quasar and AGN candidates with periodic variability, distributed over a wide redshift range up to  $z \sim 3$  ([Graham et al. 2015b](#); [Charisi et al. 2016](#); [Liu et al. 2016](#)). Due to the limited temporal baselines ( $\lesssim 10$  years), these detected rest-frame periods are confined to short time scales of several years or hundreds of days. There are also a number of quasars and nearby AGNs that were reported individually to exhibit periodicity based on long-term databases, e.g., OJ 287 ( $z = 0.31$ ; [Valtonen et al. 2008](#)), NGC 4151 ( $z = 0.003$ ; [Guo et al. 2006](#)), and NGC 5548 ( $z = 0.017$ ; [Li et al. 2016](#)). OJ 287 is long-known to have strong radio emission while NGC 4151 and NGC 5548 are marginally radio quiet ([Ho 2002](#)).

In this *Letter*, we report a possible periodicity in another

nearby galaxy Ark 120 ( $z = 0.03271^1$ ), which is a radio-quiet AGN with a radio-loudness  $R \approx 0.1$  ([Condon et al. 1998](#); [Ho 2002](#)) and 5100 Å luminosity of  $\sim 10^{44}$  erg s<sup>-1</sup> ([Peterson et al. 1998](#)). Ark 120 has long-term public photometric and spectroscopic monitoring data since 1964. We in addition made new observations between 2015-2017. The long-term variations display a sinusoidal pattern with a period of  $\sim 20$  years, which is yet the largest period among the AGNs with periodicity detected. With its plenty spectroscopically monitoring data, Ark 120 can serve as a good laboratory for studying the origin of the periodicity in general and evolution of supermassive black hole binaries in particular if the periodicity stems from the binary's orbital motion.

### 2. OBSERVATIONS AND HISTORIC DATABASE

#### 2.1. New Observations between 2015-2016

We made a two-year new observation campaign between 2015-2017 using Lijiang 2.4m telescope, located in Yunnan Province, China, operated by Yunnan Observatories. The spectrograph is equipped with a slit long enough to allow us to simultaneously observe a nearby comparison star ([Du et al. 2014](#)). We use this comparison star as a reference

<sup>1</sup> The redshift is taken from the NASA/IPAC Extragalactic Database, which yields a luminosity distance of 143 Mpc based on the *WMAP-5* cosmological parameters  $H_0 = 70.5$  km s<sup>-1</sup> Mpc<sup>-1</sup>,  $\Omega_m = 0.27$ , and  $\Omega_\Lambda = 0.73$ .

TABLE 1  
DATASETS FOR THE LIGHT CURVES OF 5100 Å CONTINUUM AND H $\beta$  FLUXES OF ARK 120.

Dataset	Ref.	Observation Periods		Number of Obs.	Aperture (arcsec)	$F([\text{O III}])^a$ ( $10^{-13} \text{ erg s}^{-1} \text{ cm}^{-2}$ )	$\varphi$	$G$ ( $10^{-15} \text{ erg s}^{-1} \text{ cm}^{-2} \text{ \AA}^{-1}$ )	Note <sup>b</sup>
		(JD-2,400,000)	(Year)						
Spectroscopy									
D99b	1	42,392-47,944	1974-1990	63	$2.0 \times 7.0$	1.35	$1.008 \pm 0.017$	$2.05 \pm 0.25$	S
P89	2	44,168-47,414	1979-1988	74	7.0	0.925	$1.005 \pm 0.021$	$1.39 \pm 0.32$	S
P98	3	47,524-50,388	1988-1996	141	$5.0 \times 7.6$	0.91	1	0	S
W96	4	48,619-48,834	1991-1992	20	$5.0 \times 10.0$	0.70	$1.078 \pm 0.005$	$0.46 \pm 0.06$	S
D08	5	48,629-53,445	1992-2005	88	$3.0 \times 11.0$	1.13	$1.037 \pm 0.003$	$0.09 \pm 0.03$	S
L	6	57,295-57,839	2015-2017	148	$2.5 \times 8.5$	0.94	...	...	S
Photometry									
P83	7	42,392-44,226	1974-1979	36	15.0	...	$0.804 \pm 0.073$	$-0.89 \pm 0.76$	V
P89	2	43,426-47,414	1977-1988	74	7.0	...	$0.540 \pm 0.301$	$5.79 \pm 0.34$	V
D99a1	8	43,963-50,818	1979-1998	25	14.3	...	$1.148 \pm 0.069$	$-5.25 \pm 0.90$	V
D99a2	8	43,079-51,186	1976-1999	50	27.5	...	$1.142 \pm 0.060$	$-8.32 \pm 0.95$	V
W92	9	47,534-48,154	1989	15	20.0	...	$0.633 \pm 0.044$	$0.53 \pm 0.77$	V
R12	10	52,207-55,644	2001-2011	54	...	...	$0.785 \pm 0.059$	$-0.08 \pm 0.86$	V
K14	11	52,237-54,319	2001-2007	67	8.3	...	$0.890 \pm 0.026$	$-0.17 \pm 0.35$	V
C	12	53,709-56,580	2005-2013	281	...	...	$0.338 \pm 0.008$	$6.81 \pm 0.12$	V

REFERENCES. — (1) Doroshenko et al. (1999b); (2) Peterson et al. (1989); (3) Peterson et al. (1998); (4) Winge et al. (1996); (5) Doroshenko et al. (2008); (6) this work; (7) Peterson et al. (1983); (8) Doroshenko & Lyuty (1999a); (9) Winkler et al. (1992); (10) Roberts & Rumstay (2012); (11) Koshida et al. (2014); (12) Catalina Survey database.

<sup>a</sup> The flux of [O III] used for absolute calibration of spectra in the dataset.

<sup>b</sup> “S” means that the fluxes are measured from spectroscopy and “V” means from V-band photometry.

standard to achieve accurate absolute and relative flux calibrations, whereas the absolute flux of the comparison star is calibrated by observations of spectrophotometric standards during nights of good weather conditions. This flux calibration method is different from the common way based on the flux constancy of narrow [O III] line as described below. However, we confirm that the narrow [O III]  $\lambda 5007$  lines of the calibrated spectra are constant with a mean of  $0.96 \times 10^{-13} \text{ erg s}^{-1} \text{ cm}^{-2}$  and a scatter within 2.5%. The slit was fixed at a projected width of  $2.5''$  and the spectra were extracted using a uniform window of  $8.5''$ . The details for the data reduction and analysis will be presented in a separate paper (Zhang, Z.-X. et al. in preparation). We obtained in total 100 spectroscopic observations, with a typical exposure of 20 minutes. The latest historic public observation was only to 2013 so that there is no temporal overlap with our observations. As a result, to align the fluxes with the historic data, we need to correct for the differences in the host galaxy contamination. Based on the two-dimensional decomposition of *HST* host galaxy image of Ark 120 by Bentz et al. (2009), we estimate the relative difference of the host galaxy contribution to 5100 Å fluxes though the apertures used in our observations and in Peterson et al. (1998) is  $\Delta F_{\text{gal}} = -(0.9 \pm 0.1) \times 10^{-15} \text{ erg s}^{-1} \text{ \AA}^{-1}$ .

## 2.2. Light Curves of 5100 Å Continuum and H $\beta$ Fluxes

Table 1 summarizes the public photometric and spectroscopic datasets to date for Ark 120 in the literature. These datasets have various apertures and different flux standards of [O III]  $\lambda 5007$  for absolute spectral calibrations. To obtain a homogeneous database, we need to intercalibrate them to correct for these differences.

For spectroscopic data, we select the dataset of Peterson et al. (1998) as a reference and scale the other datasets into a common absolute flux of [O III]  $\lambda 5007$   $F([\text{O III}]) = 0.91 \times$

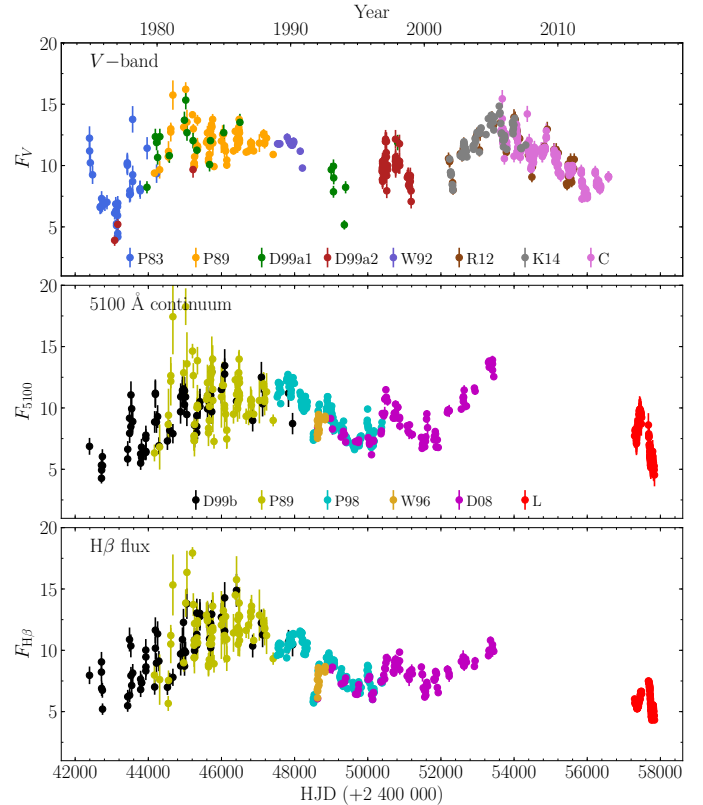


FIG. 1.— Light curves of V-band and 5100 Å continuum flux densities (in units of  $10^{-15} \text{ erg s}^{-1} \text{ cm}^{-2} \text{ \AA}^{-1}$ ), and H $\beta$  integrated fluxes (in units of  $10^{-13} \text{ erg s}^{-1} \text{ cm}^{-2}$ ) from top to bottom panels. The corresponding references of the labels are listed in Table 1.

$10^{-13} \text{ erg s}^{-1} \text{ cm}^{-2}$  because the reference dataset used<sup>2</sup>. To ac-

<sup>2</sup> It is possible that the narrow [O III] line has a long-term secular variation

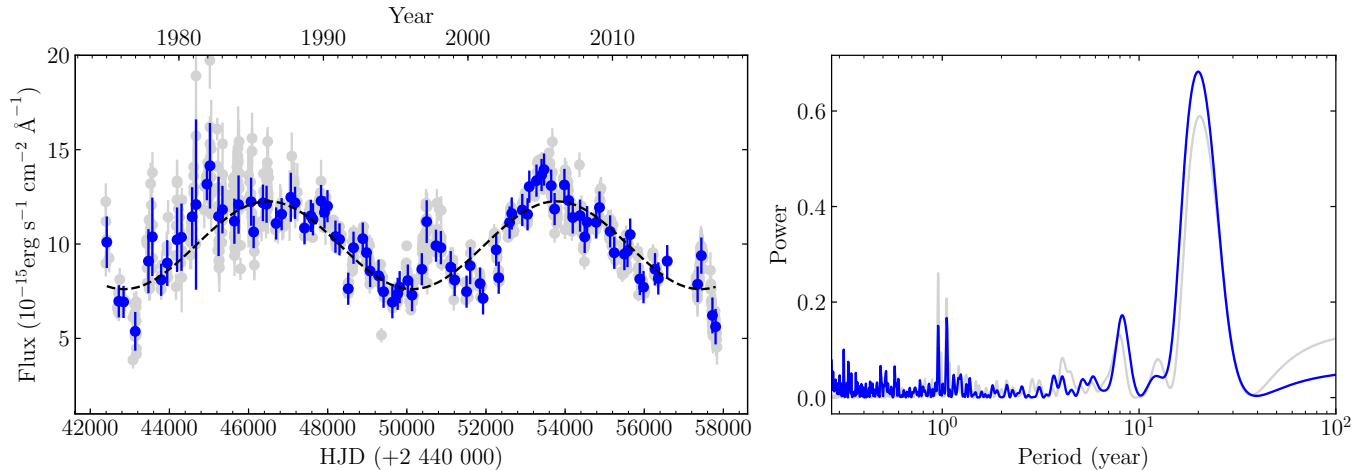


FIG. 2.— (Left) Merged light curve of  $V$ -band and  $5100 \text{ \AA}$  flux densities in gray and binned light curve with an interval of 100 days in blue. The dashed line represents the best sinusoidal fit to the binned light curve. (Right) The LS periodogram of the binned (blue) and the original (gray) light curves.

count for the different aperture sizes, we apply a scale factor  $\varphi$  and a flux modulation  $G$  to the  $5100 \text{ \AA}$  flux densities and  $H\beta$  fluxes of each dataset with respect to the reference as (e.g., Peterson et al. 1995; Li et al. 2014)

$$F_{\lambda}(5100\text{\AA}) = \varphi F_{\lambda}(5100\text{\AA})_{\text{obs}} + G, \quad (1)$$

and

$$F(H\beta) = \varphi F(H\beta)_{\text{obs}}, \quad (2)$$

The values of  $\varphi$  and  $G$  are determined by comparing the measurements of the two datasets that are closely spaced. The interval for comparison is adopted to be 50 days for the datasets D08 and W96 in Table 1, which yields a good temporal overlap. For the other two datasets (D99b and P89), there is a short interval (2 years) of temporal overlap with the other datasets. Meanwhile, the sampling of these two datasets are also poor. We thus increase the interval for comparison upto 100 days to obtain a sufficient number of nearly contemporaneous observations. We note that since we concentrate on long-term variations, the choice of the interval has no influences on our analysis. It is also worth mentioning that it is impossible to intercalibrate the  $H\beta$  fluxes of our new observations with the other datasets, because there is no temporal overlap. We present the light curve of  $H\beta$  fluxes for the purpose of illustrating the variation behaviour of  $H\beta$  line. We do not use it for subsequent periodicity analysis.

For  $V$ -band photometric data, we first convert the magnitudes into flux densities by adopting the zero point  $F_{\lambda}(V=0) = 3.92 \times 10^{-9} \text{ erg s}^{-1} \text{ cm}^{-2} \text{ \AA}^{-1}$  (Johnson 1996). We then scale the flux densities to align with the  $5100 \text{ \AA}$  flux densities by again applying a multiplicative scale factor ( $\varphi$ ) and an additive flux adjustment ( $G$ ) to bring them into a common flux scale with the light curve of  $5100 \text{ \AA}$  continuum as

$$F_{\lambda}(5100\text{\AA}) = \varphi F_{\lambda}(V)_{\text{obs}} + G. \quad (3)$$

The interval for comparison is adopted to be 50 days for all the datasets. Table 1 also lists the values of  $\varphi$  and  $G$  for all the spectroscopic and photometric datasets. In Figure 1, we

as in NGC 5548 (Peterson et al. 2013). We do not include such a variation in our intercalibration as there were no reliable absolute flux measurements over the whole period of the datasets.

plot the light curves of  $V$ -band fluxes densities,  $5100 \text{ \AA}$  flux densities, and  $H\beta$  integrated fluxes.

### 2.3. $H\beta$ Profiles

The  $H\beta$  profiles used in this work are mainly from Stanic et al. (2000) and Doroshenko et al. (2008), which presented 10 broad averaged  $H\beta$  profiles over 1977-1990 (see their Figure 3-11) and 21  $H\beta$  profiles over 1992-2005 (see their Figure 5), respectively. We digitalize these figures to obtain the profile data. Since we only concentrate on the shape of  $H\beta$  profile, the absolute fluxes is no longer important. Besides, Capriotti et al. (1982) presented 6 spectra of Ark 120 over 1976-1981, Korista (1992) presented 12 spectra over 1981-1989, and Peterson et al. (1998) presented one averaged spectra around 1993. We again digitalize them and isolate out broad  $H\beta$  profiles following the procedure in Stanic et al. (2000). The narrow  $H\beta$  line and Fe II emission are subtracted using a simple spectral decomposition (see Stanic et al. 2000 for a detail). We also supplement two mean  $H\beta$  profiles from our two-year reverberation mapping monitoring. In total, we obtain 52 profiles that cover a time span of 40 years.

## 3. PERIODICITY ANALYSIS

As shown in Figure 1, all the light curves of  $V$ -band,  $5100 \text{ \AA}$  continuum, and  $H\beta$  integrated fluxes oscillate with a roughly sinusoidal pattern. In Figure 2, we merge the light curves of  $V$ -band and  $5100 \text{ \AA}$  continuum as described above. The peaks and valleys of the sine-like variations are seen more clearly in the merged light curve. A visual inspect can find an interval of 20 years between peaks/valleys. The light curve of  $H\beta$  fluxes only covers 1.5 cycles whereas the merged light curve of  $V$ -band and  $5100 \text{ \AA}$  continuum covers more than 2 cycles. In the following, we only use the merged light curve for periodicity analysis. It is interesting to mention that there is a tiny peak in the valley around year 1996, which seems to repeat after  $\sim 20$  years, around year 2016, although the data points around 2016 is relatively sparse and there is a gap of two years to the preceding observations.

To alleviate the influences of highly irregular cadence and suppress the short-term fluctuations in the light curve, we bin the light curve with an interval of 100 days. The uncertainties of points in the newly binned light curve are assigned as follows: we first calculate the mean standard deviation of the

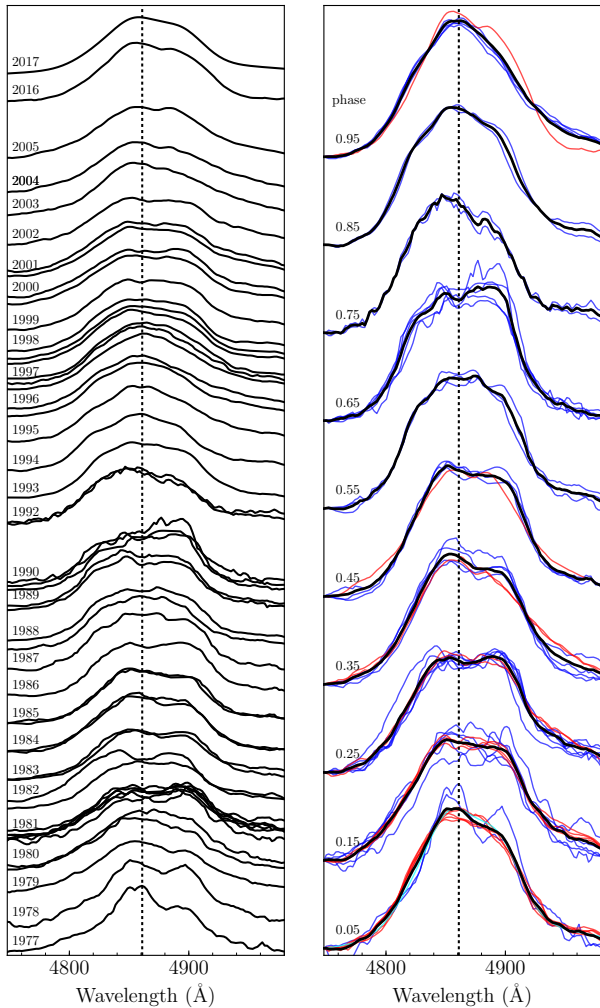


FIG. 3. — (Left)  $H\beta$  profiles from 1976 to 2017. (Right) Folded  $H\beta$  profile series with phases for a complete cycle using a period 19.96 years. Black lines represent the overall mean profiles of each phase. Blue, red, and cyan lines represent profiles from the first, second, and third cycles of the series. There is only one profile in the third cycle, which is folded into the first phase. Vertical lines show the wavelength center of  $H\beta$  line.

whole light curve, and then compare it with the standard deviations of each bin and set the corresponding uncertainty to be the maximum one. In the left panel of Figure 2, we superpose the binned light curve with blue points upon the original light curve with gray points. We use a sinusoidal curve to fit the binned light curve, leading to a period of  $19.96 \pm 0.49$  years. The fitting has a minimum  $\chi^2/\text{dof} = 1.6$ .

We also use the Lomb-Scargle (LS) periodogram to test for the periodicity in the light curve<sup>3</sup>. The right panel of Figure 2 shows the periodograms for the binned and the unbinned light curves, which peak at 19.94 and 20.30 years, respectively, consistent with the value from the sinusoidal fitting.

#### 4. $H\beta$ PROFILE VARIATIONS

Figure 3 shows the total publicly available  $H\beta$  profiles from 1976 to 2017. The profiles are highly asymmetric and have double peaks (e.g., 1981 and 1989), which seem to shift and

<sup>3</sup> We use the module `LombScargle` in the Python package `astropy` (<http://www.astropy.org>) to calculate the LS periodogram, which implements the algorithm presented by [Press & Rybicki \(1989\)](#).

merge in opposite direction. Moreover, the amplitudes of the red and blue peaks also vary independently. These strong variations of  $H\beta$  profiles potentially reflect that the  $H\beta$  broad-line region undergoes notable changes. Such behaviour is similar to that of  $H\beta$  profiles in NGC 5548 ([Li et al. 2016](#)). Unfortunately, the present database of  $H\beta$  profiles is not enough to perform an epoch folding scheme as in [Li et al. \(2016\)](#) to test for the periodicity in the line profile variations.

Nevertheless, we fold the profiles into 10 uniformly-spaced phases using a period of 19.96 years in the right panel of Figure 3. The phase bin width corresponds to  $\sim 2$  years and each phase bin has in average five profiles. It is more evident in the folded profile series that the red and blue peaks shift with phases significantly and their amplitudes vary independently. For the sake of comparison, we plot the  $H\beta$  profiles from the first cycle (1976-1995), second cycle (1996-2016), third cycle (2017-2026) in blue, red, and cyan, respectively, and the overall mean profile in black. There is only one profile in the third cycle, which is folded into the first phase. As can be seen, the profiles from three cycles are generally matched. Specifically, the separation and amplitude of the double peaks are in general agreement. This plausibly indicates that  $H\beta$  profiles may change with a similar period as the continuum.

## 5. DISCUSSIONS

### 5.1. False Positive Rate of the Periodicity

AGN variations can be described stochastically as “red noise” with a power-law shape  $P(f) \propto f^{-\alpha}$ . [Vaughan et al. \(2016\)](#) showed that such red-noise stochastic processes can also produce false positive periodicity in few-cycle light curves. Below we use Monte-Carlo simulations to calculate the false positive rate for the sampling pattern of Ark 120 following [Vaughan et al. \(2016\)](#). For simplicity, we only use the damped random walk (DRW) model to delineate the variations. The DRW process has a power spectrum ([Kelly et al. 2009](#))

$$P(f) = \frac{2\sigma^2\tau^2}{1 + (2\pi\tau f)^2}, \quad (4)$$

where  $\tau$  is the typical damping timescale and  $\sigma$  is the standard deviation of the time series over long time scale ( $\gg \tau$ ).

The binned light curve has a mean of 10.13 and a standard deviation of 2.02 (hereafter in units of  $10^{-15} \text{erg s}^{-1} \text{\AA}^{-1}$ ). We accordingly set  $\sigma = 2.02$  throughout the simulations. The typical value of  $\tau$  is largely unknown because AGNs with continuing monitoring as long as four decades is very rare. There is a number of systematic studies on AGN variability over shorter timescale ([Kelly et al. 2009](#); [MacLeod et al. 2010](#)), giving a typical timescale on the order of  $\sim 100$  days for AGNs with  $5100 \text{\AA}$  luminosities of  $10^{44} \text{erg s}^{-1}$ . This apparently cannot describe variations on a timescale of decades. On the other hand, the simulations of [Vaughan et al. \(2016\)](#) illustrated that the false positive rate depends on the measurement errors. Using unrealistically overestimated errors leads to too much “white noise” in the simulations, which reduces the probability for producing strong periodic modulations. We therefore calculate the false positive rates for a wide range of  $\tau$  and (fake) measurement noises.

With the given parameters of  $\sigma$  and  $\tau$ , we perform simulations as following steps. We first generate a mock light curve with 1000 points over the baseline same as that of Ark 120, and use linear interpolation to obtain the fake measurements at the observed times. We then scale and shift the newly gener-

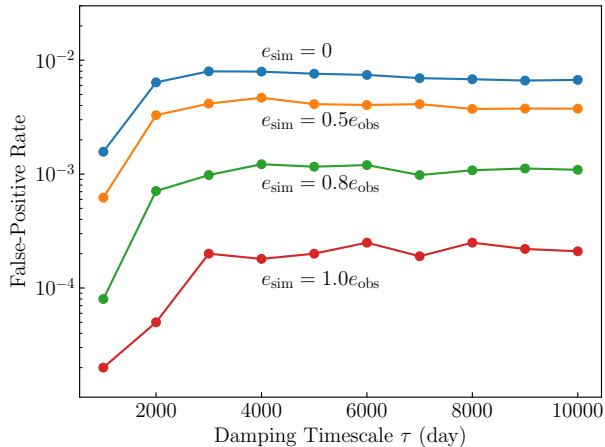


FIG. 4.— The false positive rate with the damping timescale ( $\tau$ ) in the DRW model. From top to bottom, lines represent the input noises ( $e_{\text{sim}}$ ) in simulations in term of real measurement noise ( $e_{\text{obs}}$ ):  $e_{\text{sim}} = 0$ ,  $0.5e_{\text{obs}}$ ,  $0.8e_{\text{obs}}$ , and  $1.0e_{\text{obs}}$ , respectively.

ated light curve by multiplying a factor and adding a constant to ensure the variance and mean flux equal to those of the observed data; To simulate observational noises, additional independently random, Gaussian noises are finally incorporated into the generated fluxes. Note that the final errorbars of simulated data are assigned as in the real data.

As in Section 3, we fit the fake light curve with the sinusoidal model and identify as a “periodic candidate” if the following criteria are satisfied: 1) the fit has a minimum reduced  $\chi^2/\text{dof} < 1.6$  and the improvement compared to the fit using a constant is significant with  $\Delta\chi^2 > 300$ ; and 2) the light curve covers at least 1.5 cycles. The choice of the first criterion is based on the data of Ark 120 for the purpose of selecting out light curves with significant variability. The choice of the second criterion is widely used in previous time-domain surveys (Graham et al. 2015b; Liu et al. 2016).

Figure 4 plots the false positive rates for different  $\tau$ . From top to bottom, lines represent the amount of measurement errors ( $e_{\text{obs}}$ ) incorporated into simulations:  $\sigma_{\text{sim}} = 0, 0.5, 0.8$ , and  $1.0e_{\text{obs}}$ , respectively. The rate rises rapidly from  $\tau = 1000$  to 3000 days, and then tends to be flat. As expected, the rate strongly depends on the amount of noises added in the simulations. The case without inclusion of noises gives a conservative estimate of the false positive rate  $< 1\%$ . This indicates that the probability for the periodicity in the presence of purely stochastic variations (described by the damped random walk model) is less than 1%. The present baseline only covers two cycles, therefore, continued monitoring of Ark 120 is highly required to track more cycles so as to confirm the periodicity with a higher significance level.

### 5.2. The Supermassive Black Hole Binary

As for the periodicity in AGN variations, there are indeed a variety of theoretic models/interpretations (see the discussions in Li et al. 2016, Lu et al. 2016, and Bon et al. 2016). Some of the interpretations can be directly excluded in Ark 120. The precessing jet model is implausible as Ark 120 is radio quiet; The hot spot model is also impossible because it is hard to produce such large amplitude variations. The other interpretations may be tested with the aid of high-quality reverberation mapping observations (e.g., Shen & Loeb 2010).

We defer this to a future work by making use of our Lijiang reverberation mapping data.

Ark 120 has a stellar velocity dispersion of  $\sigma_* = 192 \pm 8 \text{ km s}^{-1}$  (Woo et al. 2013), resulting in a black hole mass estimate of  $M_{\bullet} = (2.6 \pm 0.2) \times 10^8 M_{\odot}$  from the  $M_{\bullet} - \sigma_*$  relation for classic bulges (Kormendy & Ho 2013). By assuming an SMBH binary residing at the center of Ark 120, the semi-major axis of the binary’s orbit is  $a_{\bullet} = 26.5$  light-days (0.02 pc or  $32 \mu\text{as}$ ) if using 19.96 years (in the observed frame) as the orbital period. If each black hole produces radio emission, such a separation can be marginally spatially resolved by the Event Horizon Telescope with an angular resolution of  $\sim 20 \mu\text{as}$  (Fish et al. 2016).

$\text{H}\beta$  reverberation mapping observations of Ark 120 showed a typical size of 30-40 light-days for the  $\text{H}\beta$  broad-line region (Peterson et al. 1998; Zhang et al. 2017), indicating that the binary orbit is slightly smaller/comparable with the  $\text{H}\beta$  broad-line region. The interaction between the binary black holes and the broad-line regions is therefore important to shaping the broad line profiles. On the other hand, the characteristic strain amplitude of the gravitational wave emission is on the order of  $h_s \sim 10^{-17}$ , which is in the sensitivity of next-generation Pulsar Time Array (Janssen et al. 2015).

## 6. CONCLUSION

Based on our compiled historic archival photometric and spectroscopic data over four decades, we report a possible period of  $\sim 20$  years in long-term brightness variations of the nearby radio-quiet galaxy Ark 120. The variations of both the optical continuum and  $\text{H}\beta$  integrated fluxes have a sinusoidal pattern with an amplitude  $> 50\%$ . The false positive rate of the periodicity is estimated be less than 1%. Meanwhile, the broad  $\text{H}\beta$  line of Ark 120 shows double peaks, which shift and merge with time. Although the available database of  $\text{H}\beta$  profiles (only 52 profiles over 40 years) is insufficient to draw a firm conclusion, it is plausible that the  $\text{H}\beta$  profile changes with a similar period. These lines of observations makes Ark 120 to be one of the nearest AGNs with periodic variability, a remarkable analogy to NGC 5548 (Li et al. 2016). Ark 120 is therefore a plausible candidate for supermassive black hole binaries. The supermassive black hole binary system in Ark 120 can be marginally spatially resolved by the Event Horizon Telescope and its gravitational wave radiation lies within the sensitivity of next-generation Pulsar Time Array.

We acknowledge the support of the staff of the Lijiang 2.4 m telescope. Y.R.L. acknowledges financial support from the National Natural Science Foundation of China (NSFC) through grant No. 11570326 and from the Strategic Priority Research Program of the Chinese Academy of Sciences through grant No. XDB23000000. L.C.H. acknowledges financial support from the Kavli Foundation and Peking University. This research is supported in part by Grant No. 2016YFA0400700 from the Ministry of Science and Technology of China, by Grant No. QYZDJ-SSW-SLH007 from the Key Research Program of Frontier Sciences, CAS, and by NSFC grants NSFC-11173023, -11133006, -11233003, -11303026, -11573026, and -U1431228.

## REFERENCES

- Bentz, M. C., Peterson, B. M., Netzer, H., Pogge, R. W., & Vestergaard, M. 2009, *ApJ*, 697, 160
- Bon, E., Zucker, S., Netzer, H., et al. 2016, *ApJS*, 225, 29
- Capriotti, E. R., Foltz, C. B., & Peterson, B. M. 1982, *ApJ*, 261, 35
- Charisi, M., Bartos, I., Haiman, Z., et al. 2016, *MNRAS*, 463, 2145
- Condon, J. J., Yin, Q. F., Thuan, T. X., & Boller, T. 1998, *AJ*, 116, 2682
- Du, P., Hu, C., Lu, K.-X., et al. 2014, *ApJ*, 782, 45
- Doroshenko, V. T., Sergeev, S. G., & Pronik, V. I. 2008, *Astronomy Reports*, 52, 442
- Doroshenko, V. T., & Lyuty, V. M. 1999a, *Astronomy Letters*, 25, 771
- Doroshenko, V. T., Sergeev, S. G., Pronik, V. I., & Chuvayev, K. K. 1999b, *Astronomy Letters*, 25, 569
- Fish, V., Akiyama, K., Bouman, K., et al. 2016, *Galaxies*, 4, 54
- Graham, M. J., Djorgovski, S. G., Stern, D., et al. 2015a, *MNRAS*, 453, 1562
- Graham, M. J., Djorgovski, S. G., Stern, D., et al. 2015b, *Nature*, 518, 74
- Guo, D., Tao, J., & Qian, B. 2006, *PASJ*, 58, 503
- Ho, L. C. 2002, *ApJ*, 564, 120
- Janssen, G. H., et al. 2015, in *Proc. Advancing Astrophysics with the Square Kilometre Array (AASKA14)*, 37
- Johnson, H. L. 1966, *ARA&A*, 4, 193
- Kelly, B. C., Bechtold, J., & Siemiginowska, A. 2009, *ApJ*, 698, 895
- Kormendy, J., & Ho, L. C. 2013, *ARA&A*, 51, 511
- Korista, K. T. 1992, *ApJS*, 79, 285
- Koshida, S., Minezaki, T., Yoshii, Y., et al. 2014, *ApJ*, 788, 159
- Li, Y.-R., Wang, J.-M., Ho, L. C., et al. 2016, *ApJ*, 822, 4
- Li, Y.-R., Wang, J.-M., Hu, C., Du, P., & Bai, J.-M. 2014, *ApJ*, 786, L6
- Liu, T., Gezari, S., Burgett, W., et al. 2016, *ApJ*, 833, 6
- Liu, T., Gezari, S., Heinis, S., et al. 2015, *ApJ*, 803, L16
- Lu, K.-X., Li, Y.-R., Bi, S.-L., & Wang, J.-M. 2016, *MNRAS*, 459, L124
- MacLeod, C. L., Ivezić, Ž., Kochanek, C. S., et al. 2010, *ApJ*, 721, 1014
- Peterson, B. M., Denney, K. D., De Rosa, G., et al. 2013, *ApJ*, 779, 109
- Peterson, B. M., Korista, K. T., & Wagner, R. M. 1989, *AJ*, 98, 500
- Peterson, B. M., Pogge, R. W., Wanders, I., Smith, S. M., & Romanishin, W. 1995, *PASP*, 107, 579
- Peterson, B. M., Wagner, R. M., Crenshaw, D. M., et al. 1983, *AJ*, 88, 926
- Peterson, B. M., Wanders, I., Bertram, R., et al. 1998, *ApJ*, 501, 82
- Press, W. H., & Rybicki, G. B. 1989, *ApJ*, 338, 277
- Roberts, C. A., & Rumstay, K. R. 2012, *Journal of the Southeastern Association for Research in Astronomy*, 6, 47
- Shen, Y., & Loeb, A. 2010, *ApJ*, 725, 249
- Stanic, N., Popovic, L. C., Kubicela, A., & Bon, E. 2000, *Serbian Astronomical Journal*, 162, 7
- Valtonen, M. J., Lehto, H. J., Nilsson, K., et al. 2008, *Nature*, 452, 851
- Vaughan, S., Uttley, P., Markowitz, A. G., et al. 2016, *MNRAS*, 461, 3145
- Winge, C., Peterson, B. M., Pastoriza, M. G., & Storchi-Bergmann, T. 1996, *ApJ*, 469, 648
- Winkler, H., Glass, I. S., van Wyk, F., et al. 1992, *MNRAS*, 257, 659
- Woo, J.-H., Schulze, A., Park, D., et al. 2013, *ApJ*, 772, 49
- Zhang, Z.-X. et al. 2017, *ApJ* in preparation
- Zheng, Z.-Y., Butler, N. R., Shen, Y., et al. 2016, *ApJ*, 827, 56